

Nanodot Formation on the Si(111)-(7 × 7) Surface by Adatom Trapping

L. Vitali, M. G. Ramsey, and F. P. Netzer

Institut für Experimentalphysik, Karl-Franzens-Universität Graz, A-8010 Graz, Austria

(Received 16 February 1999)

The formation of a superlattice of metallic nanoclusters consisting of nine adatoms each is reported for thallium on the Si(111)-(7 × 7) surface. It is proposed that mobile adatoms are trapped in attractive potential wells on the faulted half of the (7 × 7) unit cell. Adatom-adatom and adatom-substrate interactions combine within these basins of attraction to create the observed metallic bonding situation. From quasiequilibrium thermodynamic considerations, the energy difference between adsorption on the faulted and unfaulted unit cell halves, that yields the ordered superstructure array, is estimated to 0.075 eV.

PACS numbers: 61.16.Ch, 61.46.+w, 68.35.Bs, 82.65.Dp

The controlled formation of ordered metal nanostructures on solid surfaces by self-organized growth is a fabulous challenge of both fundamental scientific and applied technological research [1]. The nucleation of adatoms into an ordered array of regular clusters of dimensions small enough that quantum mechanical effects determine their properties, i.e., quantum dots or nanodots, is of particular interest, since new properties such as quantum interference effects may emerge [1,2]. Here we describe the formation of an ordered array of two-dimensional nanodot structures of deposited metal atoms on the Si(111)-(7 × 7) surface. The process is mediated by the *intrinsic attractive potential wells* that exist on the faulted halves of the Si(7 × 7) unit cells [3], which effectively trap diffusing metal atoms to create a regular arrangement of islands of well-defined size. This island formation process appears to be controlled thermodynamically by a quasiequilibrium situation and has been discovered during adsorption studies of *thallium* on the Si(111)-(7 × 7) surface.

The bonding of adatoms on the Si(111)-(7 × 7) surface and the identification of stable binding sites as well as the determination of surface diffusion pathways are important problems of interest for the detailed understanding of the initial stages of metal-Si interface formation. Brommer *et al.* [4] have applied the concept of “local softness” within density functional theory (DFT) to predict a qualitative pattern of reactive sites for the interaction of atoms and molecules on the Si(111)-(7 × 7) surface. Within the framework of a local bonding concept adsorbate atoms are placed at various surface dangling bond sites in the (7 × 7) unit cell. A somewhat different approach has been put forward recently by Cho and Kaxiras [5,6], who studied the adsorption and diffusion of adatoms on the reconstructed Si(111) surface by DFT total-energy calculations. Their bonding picture is of a more delocalized nature and they introduce so-called *basins of attraction*, which contain stable adsorbate positions as high-coordination sites rather than surface dangling bond sites.

The experimental work which is reported in this Letter was undertaken to elucidate the effects of valency and atomic size on the bonding characteristics of metal

adatoms on the Si(111)-(7 × 7) surface reconstruction: The group III metal thallium was chosen for this purpose. The reason for this choice was that group III metals provide well-suited model systems for such studies since their interfaces to Si are nonreactive. Tl, the heaviest member of this group, is particularly interesting as it occurs in two different valencies in chemical compounds, namely, in a monovalent state in addition to the more common trivalent state, ubiquitous to other members of the group III elements [7]. As demonstrated by the scanning tunneling microscopy (STM) data presented in this Letter, we find a very unusual interface behavior of Tl on Si(111): the Tl adatoms agglomerate at room temperature into an array of well-defined nanoclusters on the (7 × 7) surface up to Tl coverages of about 0.2 monolayers. At this coverage the whole surface is uniformly covered by Tl *nanodots*, which are located on the faulted halves of the (7 × 7) unit cells. We argue that this trapping effect of adatoms is caused by the attractive potential wells on the surface, in which adatom-adatom and adatom-substrate interactions cooperate creating a metalliclike delocalized type of bonding situation. This provides a mechanism for the formation of nanodots which is *electronic* in origin, and which is contrasted with the strain-mediated nanostructure formation process as encountered in metal-on-metal systems [1].

Details of the experimental apparatus can be found in Ref. [8]. Thallium was evaporated on to clean Si(111)-(7 × 7) surfaces from a boron nitride crucible, and the evaporation rates were controlled by a quartz film thickness monitor. The Tl surface coverages have been determined from the evaporation rate and by AES in combination with STM as described elsewhere [9] [one monolayer (ML) corresponds to the site density of the unreconstructed Si(111) surface].

The constant-current topographic STM images of Figs. 1(a) and 1(b) illustrate the formation of Tl nanodots on the Si(111) surface: ~0.2 ML of Tl have been deposited at room temperature onto the Si(7 × 7) reconstruction. This surface is uniformly decorated by a regular array of two-dimensional triangular clusters, which almost

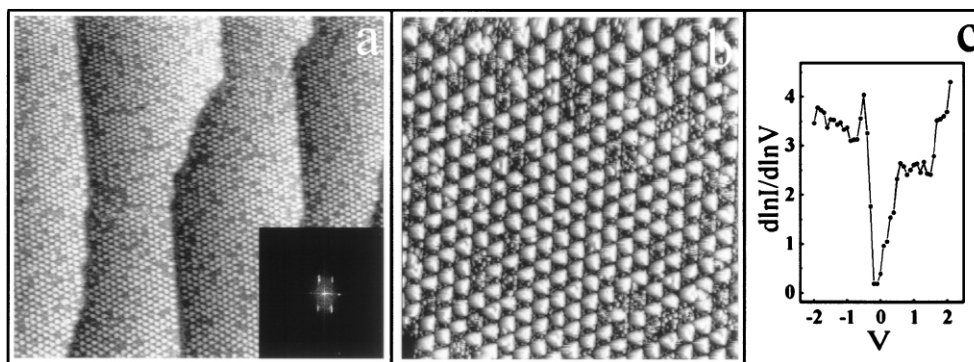


FIG. 1. Constant-current topographic STM images of Si(111)-(7 × 7) covered with ~ 0.2 ML of Tl at room temperature. (a) $1500 \times 1500 \text{ \AA}^2$; (b) $500 \times 500 \text{ \AA}^2$; tunneling conditions -2 V , 1 nA . (c) STS spectrum from the Tl clusters. The inset in (a) shows a Fourier transform of the superlattice of nanodots.

exclusively cover the faulted halves of the (7×7) unit cells. A few (7×7) unit cells remain uncovered and show up as defects in the island superlattice of Fig. 1(a). The Fourier transform of the STM image in the inset of Fig. 1(a) confirms the high degree of order and the hexagonal symmetry of the nanostructure array. The Tl nanoclusters show metallic behavior as demonstrated by the absence of a surface band gap around the Fermi energy (i.e., at 0 V) of the $d \ln I / d \ln V$ curve in the scanning tunneling spectrum (STS) of Fig. 1(c). From the absolute coverage of 0.2 ML each (7×7) unit cell half should contain on average ~ 9 Tl adatoms. It is interesting to note that individual adatoms could not be resolved in the STM images of the Tl clusters [10]. This is presumably the result of a dynamic effect caused by the high mobility of the Tl adatoms within the clusters, as discussed below.

The preferential adsorption of adatoms on the faulted halves of the Si(111)- (7×7) unit cells at low coverages has been reported for a variety of metals, such as Pb [11–13], Sn [14], Ag [15], Pd [16], and the alkali metals [17,18], but ordered superstructures have not been observed. Following the electronegativity criterion of Brommer *et al.* [4] all these metals, including Tl, have to be considered as electron donors with respect to the Si(111) surface. The local bonding considerations [4], however, provide little guidance for this situation since the DFT calculations of local softness predict preferred

reactivity of the *faulted* Si center adatoms as well as the *unfaulted* Si corner adatoms of the (7×7) unit cell towards reactants which act as donors. Therefore, it appears that the local bonding picture is unable to explain the preference of metal adatoms for the faulted (7×7) unit cell half.

The important aspect of the model of Cho and Kaxiras (CK) [5,6] for the present discussion is that metal adatoms become trapped in basins of attraction around rest atom sites (Fig. 2a), which provide stable adatom positions in terms of high coordination sites [6]; these are the T_4 -type, B_2 -type, and H_3 -type positions, which surround a central T_1 position on top of the rest atom, as shown in the schematic drawing of Fig. 2(b). The basins display threefold symmetry and contain thus three equivalent high-coordination sites each. The diffusion barriers between the T_4 -, B_2 -, and H_3 -type positions are low thus allowing for fast adatom diffusion along a closed path within the basins of attraction, but due to higher barriers surrounding the basins diffusion is slower across basins. Note that there are three basins of attraction per (7×7) half unit cell around the three Si rest atom sites. Because of the high coordination of adatoms the adsorbate bond in this model should be regarded as metallic rather than directional. The DFT calculations of CK [6] also yield much higher energies for adsorbate atoms (K, Mg, Ga, Si, and Ge) attached to dangling bond T_1 sites above intrinsic Si adatoms or rest atoms, and the possibility of

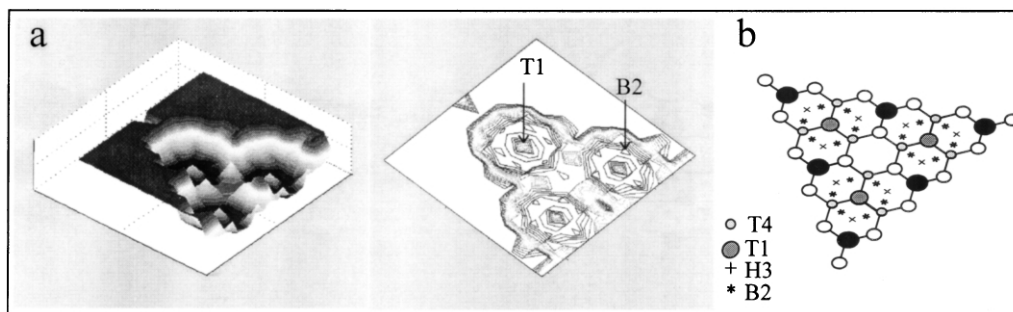


FIG. 2. Schematic drawings of the basins of attraction for adatoms in one half of the (7×7) unit cell, as adapted from Ref. [6] for K on Si(111) (a). The sites of high symmetry within the basins of attraction are indicated in (b).

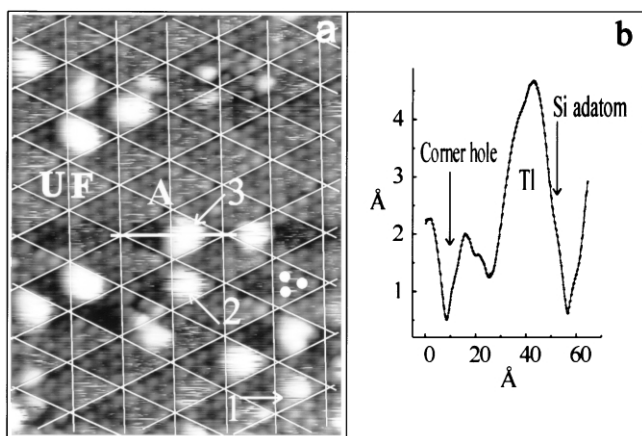


FIG. 3. (a) STM image of ~ 0.05 ML Tl on Si(111)-(7 \times 7) ($200 \times 150 \text{ \AA}^2$; -1.7 V , 1.5 nA). The faulted (*F*) and unfaulted (*U*) unit cell halves are indicated and the three basins of attraction are marked in one unit cell by the white dots. The numbers give the occupation of basins of attraction (see text). (b) Line scan along *A* in image (a).

their population by adsorbate atoms has therefore been disregarded.

The CK model, if applied to the faulted half of the (7 \times 7) unit cell, is able to explain some STM observations of Tl on Si(111) at low coverages. Figure 3(a) shows an STM image of ~ 0.05 ML of Tl on Si(111)-(7 \times 7) deposited at room temperature. A (7 \times 7) mesh has been superimposed on the image, where the CK basins of attraction around the rest atom positions are indicated by the dots in one of the unit cells. The Tl adatoms are identified as the bright blobs, their tendency to clustering is evident, and the majority of Tl adatoms concentrate on the faulted unit cell halves. We notice that the Tl STM signature in Fig. 3(a) is most naturally realized, if Tl adatoms populate 1, 2, or 3 basins of attraction in the various unit cells, as indicated by the numbers on the figure. CK have calculated theoretical STM images for a Si extra adatom in one basin of attraction [5]. The present experiment shows a remarkable similarity with the CK simulation, taking into account that the potential well for the Tl adatom is expected to be different in detail from that of the Si adatom. The line scan in Fig. 3(b), taken along the line marked *A* in the image 3(a), shows an apparent height difference of $\sim 4 \text{ \AA}$ between the Tl cluster and the corner hole of the Si(7 \times 7) unit cell. An interesting feature in Fig. 3(b) is the shoulder observed in the vertex of the (7 \times 7) unit cell. We associate this shoulder with a Si corner adatom, which forms the boundary of a basin of attraction. The Si adatoms are apparently $\sim 2.5 \text{ \AA}$ lower than the Tl cluster. Assuming a “geometrical size” of $\sim 3.4 \text{ \AA}$ for the Tl atom [19], the location of Tl adatoms in their basin of attraction is estimated to be $\sim 0.6 \text{ \AA}$ above the Si corner hole or $\sim 0.9 \text{ \AA}$ lower than the Si adatoms, if electronic effects are neglected in this estimate.

The basic idea of the CK model, attractive potential wells which act as sinks for trapping adatoms without

pronounced directional bonding, is an interesting concept for various metals on Si(111) at low adsorbate coverages. However, it is insufficient to explain (i) the preference of some metals to accommodate on the faulted half of the (7 \times 7) unit cell, and (ii) the tendency to agglomerate, as seen very clearly here for Tl on Si(111) and also observed for a number of other metal-on-Si systems [11,13,15,17,18]. In the CK calculations [5,6] the stacking fault has not been considered, and the model has been restricted to single adatoms. On a different line, Sonnet *et al.* [20] have recently applied the semiempirical crystalline extension of the extended Hückel theory (EHT) to the initial stages of Pb chemisorption on Si(111)-(7 \times 7). Sonnet *et al.* included both halves of the (7 \times 7) unit cell in the calculations and addressed explicitly the interactions between adatoms. The EHT results emphasize a tendency for metal cluster formation as a result of strong Pb-Pb interactions and favor the adsorption of Pb on the faulted half unit cell, by about 0.1 eV [20].

Keeping these results in mind, we propose the following phenomenological scenario for the formation of Tl nanoclusters on the Si(111)-(7 \times 7) surface. Attractive potential wells exist on the faulted halves of the Si(7 \times 7) unit cells, consisting of three CK basins of attraction each, which act as effective traps for the Tl adatoms. Attractive Tl-Tl interactions lead to multiple occupation of the potential basins, with up to a maximum of three adatoms per basin in accord with the threefold symmetry of the potential, yielding nine Tl adatoms per Tl cluster at saturation on every half unit cell. The adatoms are mobile within the potential wells, but the outdiffusion from the wells is restricted by the boundaries of the (7 \times 7) unit cells, the Si dimer rows, which provide a repulsive potential for adatom interaction (see below). Exchange between adjacent potential traps is inhibited with increasing population, providing a confinement effect which leads to the superlattice of nanostructures as observed in Fig. 1.

The Tl clusters are, however, mobile at room temperature for low coverages, i.e., at coverages at which neighboring empty potential wells are available at the surface. Figure 4 shows two consecutive STM images for ~ 0.05 ML of Tl, taken within 200 sec from each other on the same area of the surface, which is identified by the characteristic defects marked *D* on the two images. Concentrating on the area within the white rectangular frame, we note that three clusters (arrows) have moved their position between the two images. A detailed analysis of the mechanism of cluster migration is beyond the scope of this paper, but it seems plausible that the clusters diffuse via two-dimensional evaporation of adatoms from the cluster followed by adatom diffusion, until reassembly occurs in a different potential well (in a different unit cell) by adatom trapping. Within the present context, however, the cluster mobility is of interest from a different viewpoint: It indicates that the surface is thermodynamically under quasiequilibrium conditions. This situation allows us to estimate the energy difference of Tl adsorption

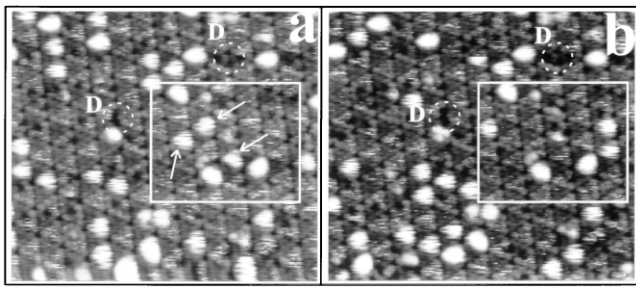


FIG. 4. STM images of ~ 0.05 ML Tl on Si(111)-(7 \times 7), room temperature ($415 \times 300 \text{ \AA}^2$; -2 V , 0.5 nA). Image (b) has been taken 200 sec after image (a) from the same area. The dashed circles *D* mark the same characteristic defects in the two images.

between the two halves of the (7 \times 7) unit cell by applying the Boltzmann distribution,

$$R = N_F/N_U = \exp(-\Delta E/kT),$$

with R denoting the ratio of the occupation numbers of faulted (N_F) and unfaulted (N_U) unit cell halves at temperature T , ΔE the energy difference, and k the Boltzmann constant. The occupation numbers obtained from the STM images yield $R = 20 \pm 5$ and $\Delta E = 0.075 \pm 0.01 \text{ eV}$. This energy difference between adsorption sites on faulted and unfaulted halves of the (7 \times 7) surface lies between those for Pb obtained experimentally by Tang *et al.* of 0.05 eV [12] and of 0.1 eV calculated by Sonnet *et al.* [20]. Given that Pb does not form an ordered array the value obtained here suggests the minimum energy difference required to form an ordered superstructure array.

Interestingly, for coverages beyond that for the ordered nanodot array the nature of the trapping potential is radically changed. This is illustrated in Fig. 5 by the comparison of an image at (a) 0.2 ML to that of (b) 0.3 ML, where the unfaulted halves of the 7 \times 7 unit cell are also significantly populated. Not only does populating the unfaulted halves destroy the nanodot superlattice, but also the nine atom clusters on the faulted halves lose their regular shape with intensity shifting towards the cell boundaries creating V shaped structures. Clearly the adsorption energy associated with the additional Tl destabilizes the adatom array, and there is a significant change in the electronic structure of the surface. However, the dimer walls of the (7 \times 7) unit cells remain clear of Tl adatoms. This repulsive potential of the dimer rows is retained even when both faulted and unfaulted halves are covered (0.7 ML, not shown).

In summary, we have observed by STM the formation of a metallic nanodot phase of Tl adatoms on the Si(111)-(7 \times 7) surface. This observation has been phenomenologically described by a model, which relies on adatom trapping in attractive potential wells on the faulted halves of the (7 \times 7) unit cells. The adatoms are selectively confined in each faulted half unit cell by three basins of attraction, which contain high-coordination sites for adatom bonding as conceptualized by Cho and Kaxiras

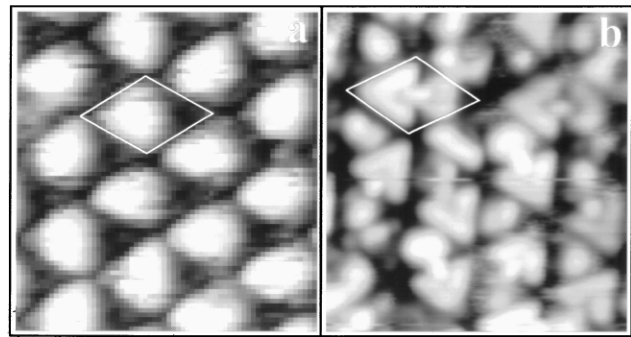


FIG. 5. STM images of ~ 0.2 ML (a) and ~ 0.3 ML Tl (b) on Si(111). [$105 \times 110 \text{ \AA}^2$; (a) -1 V , 5 nA ; (b) -1.3 V , 1.4 nA]. A (7 \times 7) unit cell is shown in both frames.

[5,6]. Adatom-substrate and adatom-adatom interactions combine to create a delocalized metallic-type bonding situation, which provides an electronic potential mechanism for the formation of a nanodot superlattice. The detailed potential balance on the Si(111)-(7 \times 7) surface appears to be particularly favorable for the trapping of Tl adatoms into an ordered array of nanostructures, but we believe that a similar type of bonding is of a more general nature and can be used to explain results seen in many metal-on-Si systems at low adsorbate coverages.

This experimental program has been supported by the Jubiläumsfonds of the Austrian Nationalbank.

-
- [1] See H. Brune *et al.*, Nature (London) **394**, 451 (1998), and references therein.
 - [2] I. B. Altfeder *et al.*, Phys. Rev. Lett. **78**, 2815 (1997).
 - [3] K. Takayanagi *et al.*, J. Vac. Sci. Technol. A **3**, 1502 (1981).
 - [4] K. D. Brommer *et al.*, Surf. Sci. **314**, 57 (1994).
 - [5] K. Cho and E. Kaxiras, Europhys. Lett. **39**, 287 (1997).
 - [6] K. Cho and E. Kaxiras, Surf. Sci. **396**, L261 (1998).
 - [7] F. A. Cotton and G. Wilkinson, *Advanced Inorganic Chemistry* (Wiley, New York, 1988).
 - [8] L. Vitali *et al.*, Phys. Rev. B **57**, 15 376 (1998).
 - [9] L. Vitali *et al.*, J. Vac. Sci. Technol. (to be published).
 - [10] The absence of atomic resolution in the STM images of the Tl nanoclusters is not due to poor instrumental resolution, since a Tl-Si (1 \times 1) monolayer phase, obtained at elevated temperature, could be readily imaged with atomic resolution (Ref. [9]).
 - [11] E. Ganz *et al.*, Phys. Rev. B **43**, 7316 (1991).
 - [12] D. Tang *et al.*, Phys. Rev. B **52**, 1481 (1995).
 - [13] J. M. Gomez-Rodriguez *et al.*, Phys. Rev. Lett. **76**, 799 (1996).
 - [14] X. F. Lin *et al.*, Surf. Sci. **366**, 51 (1996).
 - [15] S. Tosch and H. Neddermeyer, Phys. Rev. Lett. **61**, 349 (1988).
 - [16] U. K. Kohler *et al.*, Phys. Rev. Lett. **60**, 2499 (1988).
 - [17] T. Hashizume *et al.*, J. Vac. Sci. Technol. B **9**, 745 (1991).
 - [18] A. Watanabe *et al.*, Jpn. J. Appl. Phys. **37**, 3778 (1998).
 - [19] C. Kittel, *Introduction to Solid State Physics* (Wiley, New York, 1996).
 - [20] Ph. Sonnet *et al.*, Surf. Sci. **407**, 121 (1998).